The two types of 3-dehydroquinase have distinct structures but catalyze the same overall reaction

David G. Gourley[1–,3], Annette K. Shrive[1,4,5], Igor Polikarpov[1,4,6], Tino Krell[2,7], John R. Coggins[2], Alastair R. Hawkins[8], Neil W. Isaacs[9] and Lindsay Sawyer[4]

[1]These authors contributed equally to this work. [2]Division of Biochemistry and Molecular Biology, Institute of Biomedical and Life Sciences, University of Glasgow, Glasgow G12 8QQ, Scotland, UK. [3]Present address: Biochemistry Department, University of Dundee, Dundee, DD1 4HN, UK. [4]Structural Biochemistry Group, ICMB, University of Edinburgh, Michael Swann Building, King's Buildings, Mayfield Road, Edinburgh EH9 3JR, UK. [5]Present address: Physics Department, Keele University, Keele, Staffs ST5 5BG, UK. [6]Present address: LNLS, C.P. 6192, 13083-970 Campinas, Brazil. [7]Present address: Institute of Biology & Chemistry of Proteins, CNRS-UPR 412, 69367 Lyon, France. [8]Department of Biochemistry and Genetics, New Medical School, Framlington Place, University of Newcastle upon Tyne, Newcastle upon Tyne NE2 4HH, UK. [9]Department of Chemistry, University of Glasgow, Glasgow G12 8QQ, Scotland, UK.

The structures of enzymes catalyzing the reactions in central metabolic pathways are generally well conserved as are their catalytic mechanisms. The two types of 3-dehydroquinate dehydratase (DHQase) are therefore most unusual since they are unrelated at the sequence level and they utilize completely different mechanisms to catalyze the same overall reaction. The type I enzymes catalyze a *cis*-dehydration of 3-dehydroquinate via a covalent imine intermediate, while the type II enzymes catalyze a *trans*-dehydration via an enolate intermediate. Here we report the three-dimensional structures of a representative member of each type of biosynthetic DHQase. Both enzymes function as part of the shikimate pathway, which is essential in microorganisms and plants for the biosynthesis of aromatic compounds including folate, ubiquinone and the aromatic amino acids. An explanation for the presence of two different enzymes catalyzing the same reaction is presented. The absence of the shikimate pathway in animals makes it an attractive target for antimicrobial agents. The availability of these two structures opens the way for the design of highly specific enzyme inhibitors with potential importance as selective therapeutic agents.

The covalent intermediate in the type I DHQase reaction (Fig. 1) can be trapped by borohydride reduction[1]. The trapped enzyme–product complex of the type I DHQase of the human pathogen *Salmonella typhi* has been crystallized[2] and its structure solved by multiple isomorphous replacement (MIR) to 2.1 Å resolution (Table 1). The structure of the type II DHQase from another human pathogen *Mycobacterium tuberculosis* has also been solved using MIR to 2.0 Å resolution (Table 1). A stereo-diagram of typical electron density from the two structure determinations is shown in Fig. 2.

Both types of DHQase have completely different subunit architectures (Fig. 3). The overall topology of the type I DHQase is an eight-stranded α/β-barrel, a very common fold that was first reported for triose phosphate isomerase[3]. This parallel α/β-barrel arrangement has been found in other enzymes that form an imine intermediate like the class I aldolases[4], *N*-acetylneuraminate lyase[5] and dihydrodipicolinate synthase[6]. In contrast, the type II DHQase subunit consists of a five-stranded parallel β-sheet core flanked by four α-helices (Fig. 3*c*) arranged with a similar overall topology to flavodoxin[7].

The type I DHQase is a dimer with helices F, G and H at the dimer interface (Figs 3*a*, 4*a*). Interestingly Arg 213, the key residue for carboxylate recognition, previously identified by chemical modification studies[8], is located on the distorted helix G at the subunit interface. The covalently linked product is at the center of the barrel attached to Lys 170, which is located on β-strand f (Fig. 3*a*) as it is in several of the other Schiff base-dependent enzymes[4–6] but not in transaldolase where the active site lysine is on strand d rather than strand f (ref. 9). The g-G region has several interactions that distort the protein chain. Met 203 and Met 205, whose side chains both point into the active site near the substrate carboxylate, produce a main chain distortion at Ser 204. Ala 206 at the start of helix G adopts an epsilon conformation that allows the neighboring Lys 207 to make a salt bridge with the C-terminal carboxylate of Ala 252 from the other subunit. The presence of Gly 209 and Gly 216 within the G helix distorts it, and the substrate-coordinating, conserved Arg 213 is located in the helix between these two glycines. The dimeric nature of the cross-linking of the G and H helices stabilizes both the dimer and the C-terminal helix, and may help the h-H loop to maintain its conformation. This loop contains a conserved sequence that includes Gln 236 and Ser 232, which interact with the substrate carboxylate and the C-5 hydroxyl group, respectively. The remaining helices F at the dimer interface interact symmetrically with each other, with His 179 from one subunit interacting with Glu 190 and Gln 193 from the other. The main chain conformation of the neighboring residue, His 194, is distorted, although crystal contacts may also be a contributing

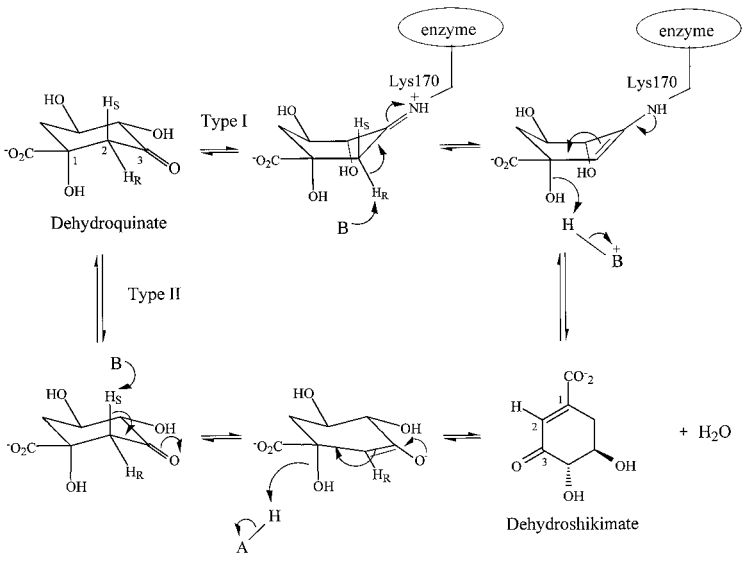

Fig. 1 The different stereochemistry and reaction mechanisms of the type I and II DHQases. The water molecule associated with the formation and breakdown of the imine (Schiff base) intermediate in the type I reaction scheme is not shown.

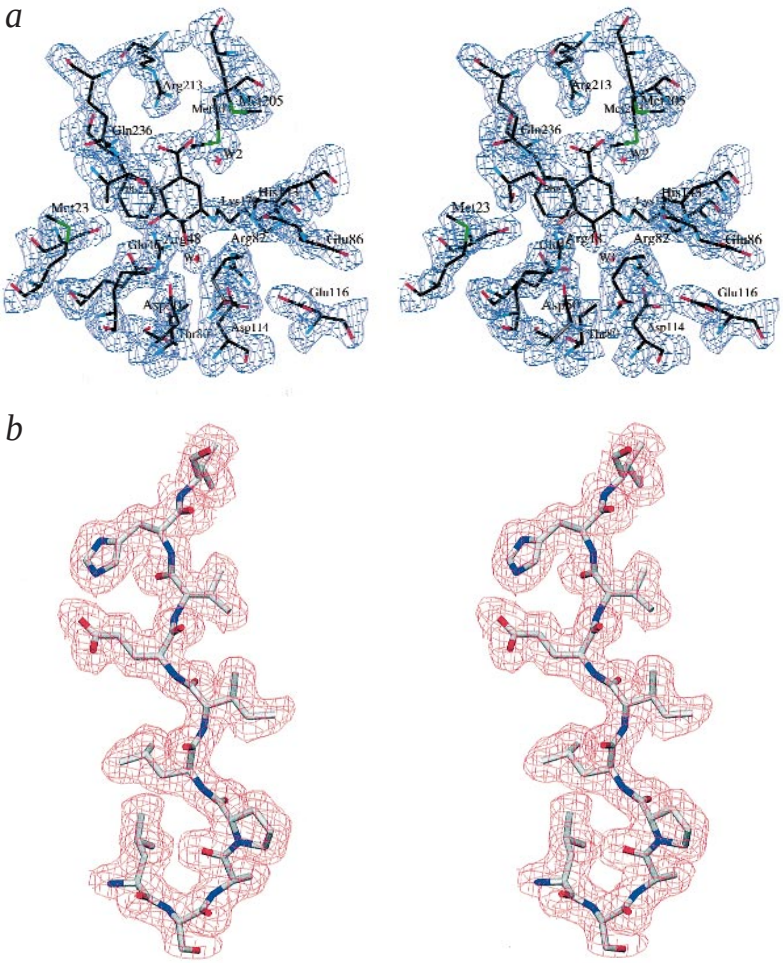

Fig. 2 Stereodiagrams of the electron density maps for the types I and II 3-dehydroquinase. ***a***, A view of the active site region within the β-barrel, looking into the site from the more open end of the barrel. The electron density map ($2F_o$ - F_c) calculated at 2.7 Å resolution is noncrystallographically averaged and solvent flattened and contoured at 1σ. The bound product is attached to Lys 170 at the C-3 position. The substrate-interacting residues Gln 236, Ser 232, Glu 46, Arg 48 and Arg 82 arise from the β-strands and the loop regions of the C-terminal end of the strands, whereas Arg 213 is located on the G helix. The water molecule W1, which interacts with the C-4 hydroxyl group and the Schiff base nitrogen of Lys 170, is also shown. ***b***, A view of the region around His 132 showing the typical quality of the ($2F_o$ - F_c) electron density map for the type II 3-dehydroquinase. There is no significant electron density for residues in the loop between Arg 18 and Gly 25.

factor. The interactions at the dimer interface and their juxtaposition to the active site may explain the observed increase in stability of the protein following borohydride reduction of the product[10].

Chemical modification and site-directed mutagenesis experiments have suggested a role for a histidine residue (His 143) as a general base abstracting the C-2 proton[11,12]. His 143 is positioned to interact with Glu 86 through the protonated nitrogen Nδ1. Glu 86 is strictly conserved in the monomeric type I DHQases, suggesting an important functional role for the glutamate, perhaps in orienting His 143 in a manner reminiscent of the serine proteases. Highly conserved side chains from different regions of the protein orient the substrate and place His 143 proximal to the C-2 side of the substrate. The C-1 carboxylate binds to Arg 213 and Gln 236 while Glu 46, Arg 48 and Arg 82 share interactions with the C-4 and C-5 hydroxyl groups. Access to the active site from the N-terminal end of the barrel is blocked by a β-hairpin, strands a1 and a2, and the substrate is stacked parallel to Phe 225, which is also in the lower, N-terminal side. The effect of this is to block any attack on the substrate from below so that the *cis* elimination mechanism for water is the only one possible.

In the type II DHQase the strand order of the β-sheet is 2, 1, 3, 4, and 5 and the connections of the successive β/α units follow the standard right-handed rule, which means that helices 2 and 3 are on one side of the sheet and helices 1 and 4 are on the other. The break in the polypeptide chain (Fig. 3*c*) is due to weak electron density for residues 19–24. These residues form a flexible loop as suggested by earlier limited proteolysis studies carried out on the enzyme in the absence of substrate[13]. The position of the active site was suggested by the cluster of conserved residues near the C-termini of the β-strands 3, 4, and 5 (Fig. 3*c*). Two residues, Arg 19 and Tyr 24[8], have been identified in earlier chemical modification and site-directed mutagenesis studies as being essential for enzyme activity. Both of these residues are on the flexible loop but modeling studies indicate that they can be readily fitted near the cluster of conserved residues. It has been proposed that the type II DHQases utilize a stepwise E_1CB (elimination unimolecular via conjugate base) mechanism involving an enolate intermediate[14] (Fig. 1). This mechanism requires base-catalyzed abstraction of the axial proton at C2 leading to enolate formation followed by the acid-catalyzed removal of the hydroxyl group at the C1 position[14] and the formation of product.

It is possible to assign roles for the conserved active site residues. His 101 is likely to be involved in abstracting the axial hydrogen at C2; its basicity would be elevated by the proximity of the carboxylate side chain of the conserved Glu 99, which forms a hydrogen bond with the Nε2 atom of His 101. Site-directed mutagenesis has already indicated that Arg 19 has a catalytic role and is therefore likely to be involved in stabilization of the enolate intermediate[8,14]. Arg 108 is in a suitable position to bind the substrate carboxylate. The side chain involved in the acid-catalyzed removal of the hydroxyl at C1 has not yet been identified. In addition, roles have not yet been assigned for the other conserved active site residues Tyr 24, His 81 and Asn 75. The latter might be involved in binding the hydroxyl groups of the substrate.

In the dodecamer, the subunits of the type II DHQase are arranged tetrahedrally as a tetramer of trimers with 23 symmetry (Fig. 4*b*). Within each trimer there are strong electrostatic interactions. A single monomer is in contact with each three-fold symmetry-related subunit via five salt bridges. The two-fold interactions (between the trimers) principally involve main-chain hydrogen bonding between the two C-terminal β-strands, which, interestingly, have the palindromic sequence Gly-Val-Ile-Val-Gly (residues 123–127). The isoleucine in this sequence is at the center of the two-fold symmetry and the palindromic arrangement provides optimal stacking of the hydrophobic side chains. In agreement with these structural observations, dissociation of the dodecameric enzyme with guanidine hydrochloride first produces a trimeric species[15].

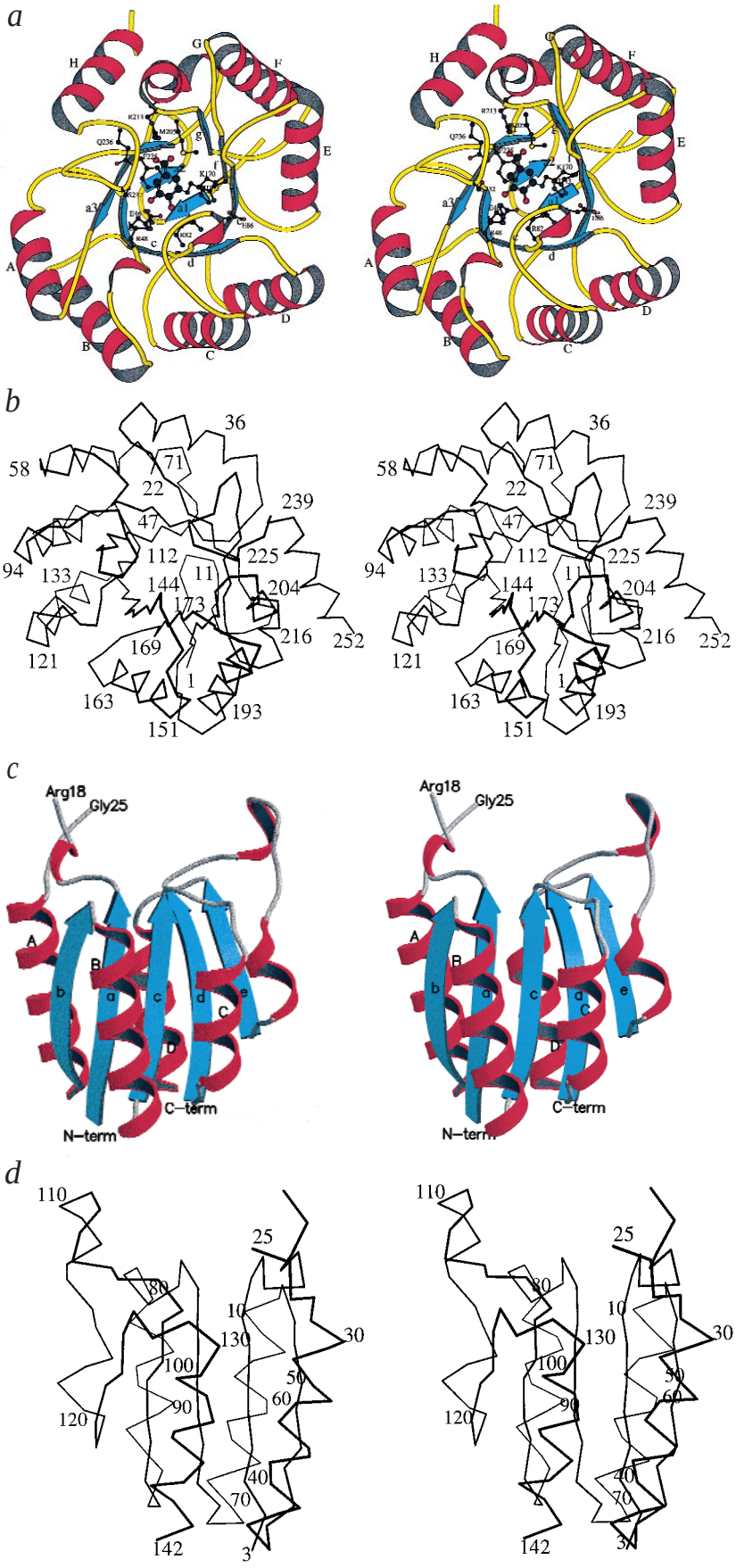

Fig. 3 The structure of an enzyme subunit. ***a***, A cartoon of the type I DHQase from *Salmonella typhi,* looking into the parallel α/β barrel. The product 3-dehydroshikimate is shown in the center of the molecule with the position of the imine-forming Lys 170 to which it is covalently attached, and the conserved side-chains involved in ligand binding, also shown. ***b***, A stereodiagram of the Cα trace of the type I DHQase subunit. ***c***, A cartoon of the type II DHQase from *Mycobacterium tuberculosis*; residues 19–24 were not included in the molecular structure since there was insufficient electron density, indicating that this region is disordered. ***d***, A stereo diagram of the Cα trace of the type II DHQase subunit. The diagrams were prepared using MOLSCRIPT[40].

The two DHQases described in this paper are both components of the biosynthetic shikimate pathway, and it is interesting to consider why there might be two structurally and mechanistically distinct forms of this enzyme. The type I DHQases are found in plants, fungi and many bacterial species including archaebacteria, and are exclusively biosynthetic. The type II enzymes are either part of the shikimate pathway or form part of the quinic acid utilization (*qut*) pathway, which shares a common biochemical step with the shikimate pathway[16]. The catabolic *qut* pathway[17,18], which occurs in saprophytic fungi such as *Neurospora crassa* and *Aspergillus nidulans*, provides a route for the conversion of the abundant plant storage compound quinic acid (or its esters) into succinyl CoA for use as a major source of carbon and energy. The biosynthetic type II enzymes occur in many bacterial species including *M. tuberculosis, Streptomyces coelicolor* and *Helicobacter pylori*. The *qut* pathway, which depends on a storage compound produced by higher plants, must have evolved later than the shikimate pathway, which was essential from the earlier stages of evolution for the production of key aromatic compounds including amino acids and ubiquinone. We propose that the first type II DHQases were new enzymes that were laterally recruited from an unknown ancestor to permit a saprophytic adaptation to the appearance of an abundant plant storage compound. Initially these type II DHQases were exclusively catabolic, but later they were used in a biosynthetic role in some species. This is consistent with the occurrence of both a biosynthetic type I DHQase and a catabolic type II DHQase in fungi such as *N. crassa*[19] and *A. nidulans*[20]. It also explains the presence of a single dual- function type II DHQase in *Amycolatopsis methanolica*[21], which appears to have lost the ancestral type I enzyme. Evidence from sequencing of the complete genomes of *M. tuberculosis*[22] and *H. pylori*[23] indicates that these species have also lost the type I DHQase and have only a type

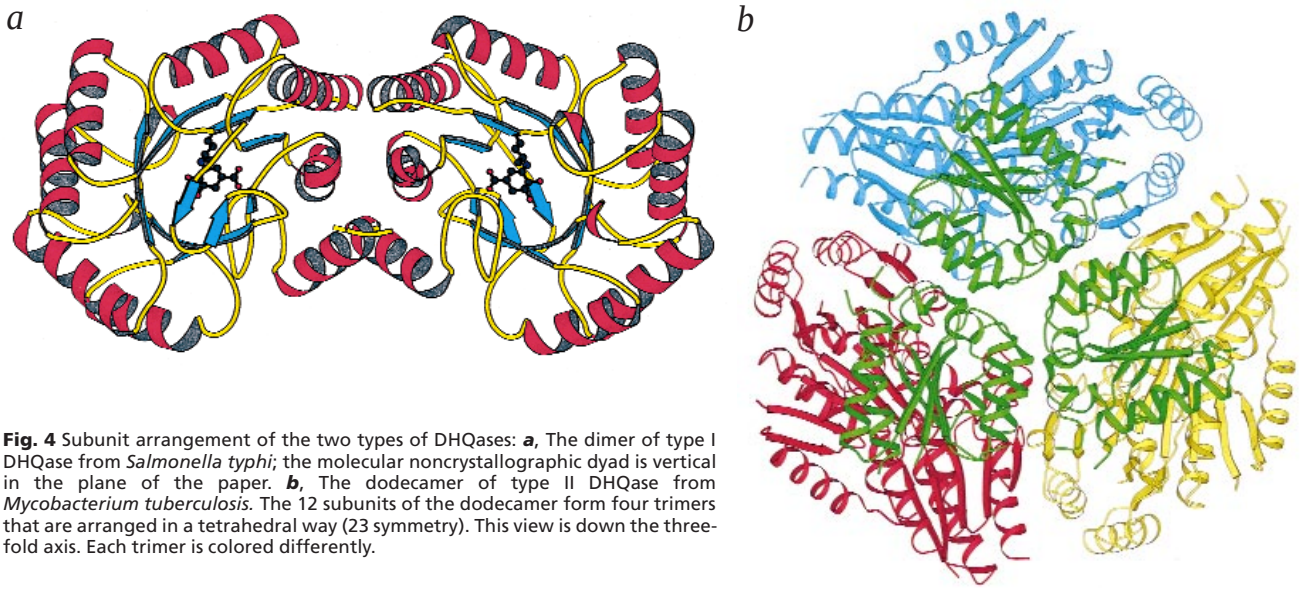

Fig. 4 Subunit arrangement of the two types of DHQases: ***a***, The dimer of type I DHQase from *Salmonella typhi*; the molecular noncrystallographic dyad is vertical in the plane of the paper. ***b***, The dodecamer of type II DHQase from *Mycobacterium tuberculosis.* The 12 subunits of the dodecamer form four trimers that are arranged in a tetrahedral way (23 symmetry). This view is down the three-fold axis. Each trimer is colored differently.

II DHQase gene. It is also interesting to note that in *N. crassa*[19] and *A. nidulans*[20], transcriptional control of the quinate catabolic pathway is provided by activator (QA-1F[17], QUTA[16]) and repressor (QA-1S[17], QUTR[16]) proteins that are clearly related to the multidomain AROM complex that is responsible for five of the seven enzymatic activities making up the shikimate biosynthetic pathway[16,17,24].

The shikimate pathway is essential for the growth of microorganisms and plants, but it is absent in animals[25]. The commercial success of glyphosate as a broad-spectrum post emergence herbicide has already established that the shikimate pathway enzymes are excellent targets for herbicides[26]. The pathway enzymes have also been proposed as targets for antimicrobial agents[27] with (6S)-6-fluoroshikimic acid already having been shown to be active against aromatic biosynthesis[28]. Further, *aroD* strains that lack the type I DHQase gene, from both *S. typhi*[29] (in fact, an *aroC aroD* double mutant) and *Shigella flexneri*[30] have been shown to make satisfactory live oral vaccines, the latter providing monkeys with protection against oral challenge with live *S. flexneri* 2457T. The availability of the structures of both types of DHQases now opens the way for the structural design of inhibitors of this earlier step in the pathway. The fact that there are two mechanistically distinct forms of DHQase may allow the development of selective inhibitors for the two types of enzyme. This could be valuable in the selective therapy of slowly growing organisms such as *M. tuberculosis* and *H. pylori*, which have only the type II enzymes, in contrast with gut organisms such as *Escherichia coli*, which have type I enzymes only.

Methods

Type I DHQase. Significant polymorphism between native and heavy-atom crystals as well as among native crystals themselves hindered the structure solution. However, monoclinic crystals of enzyme inactivated by treatment with dehydroquinate and sodium borohydride were grown in space group $P2_1$ with a = 60.49, b = 45.39, c = 85.47 Å, β = 95.48°, Z = 2 and a solvent content of 42% (ref. 2). The data were processed using DENZO[31], and the structure solution and subsequent refinement of the structure were carried out using programs from the CCP4 suite[32] and X-PLOR[33]. Heavy-atom sites were determined from difference Patterson maps and refined with VECREF and then MLPHARE[34]. A final multiple isomorphous replacement (MIR) map was calculated to 2.7 Å resolution and the phasing analysis gave a figure of merit of 0.74. The map was solvent flattened using the program DM[35], and the polypeptide chain was traced using both the map at 2.7 Å resolution and a low-resolution (17–3.5 Å) map. Model building was carried out using the program O[36]. Following a successful tracing of both independent molecules, further maps were averaged in DM. Manual alignment of the sequence in the electron density positioned the proposed imine-forming residue Lys 170 in close proximity to electron density associated with the bound substrate. Cycles of model building, phase combination with the MIR phases, solvent flattening, symmetry averaging and calculation of electron density maps were carried out until all the residues and protein electron density were successfully fitted. No further phase combination was then carried out and the independent molecules were fitted individually. Positional refinement and simulated annealing were performed using all of the data, initially in the range 12.0–3.5 Å and gradually extended to 2.1 Å, using two-fold noncrystallographic restraints throughout. The imine-linked substrate and 137 water molecules were added. Final refinement included individual isotropic B refinement but the noncrystallographic restraints were not released. There were no detectable differences between the two independent molecules other than side chains involved in crystal contacts (main chain + Cβ r.m.s. = 0.041 Å). The average B-factor (all atoms) is 22.2 $Å^2$.

Type II DHQase. DHQase from *M. tuberculosis* was purified and crystallized as described[37]. Single-wavelength X-ray data were recorded from crystals mounted in capillaries, as crystals were relatively insensitive to radiation damage. The enzyme crystallized in space group F23 with cell dimensions a = b = c = 127.9 Å. The asymmetric unit contains a single enzyme subunit. Derivatives were obtained by soaking potassium tetrachloroplatinate and mercury cyanide, and MIRAS phases (multiple isomorphous replacement with anomalous scattering) were calculated and refined using MLPHARE[34]. Although the two mercury derivatives (1 and 2) had identical mercury positions, they were treated as independent derivatives since they differed in the mercury occupation. Electron density maps calculated using both mercury derivatives were better than maps computed from phases calculated from only one mercury data set. The overall figure of merit for the MIRAS phasing was 0.4 for acentric reflection and 0.6 for centric reflections for data from 10 to 2.2 Å. Density modification with DM[35] gave an interpretable map. After a Cα trace was fitted into the MIRAS map using bones generated by the program O[36], a polyalanine trace was built consisting of three polypeptide segments of 118 residues in total. The first model had ~80% of the alanine residues replaced with the correct side chains and was then subjected to rounds of refinement with REFMAC[38] and model building with O. In the refinement, data were

Table 1 Crystallographic data and statistics for type I DHQase from *S. typhi* and type II DHQase from *M. tuberculosis*

	Type I DHQase						Type II DHQase				
	Native	$K_2Pt(NO_2)_4$	$HgCl_2$	K_2PtCl_6	$K_2Pt(NO_2)_4$	$UO_2(NO_3)$	Native (1)	Native (2)	$Hg(CN)_2$ (1)	$Hg(CN)_2$ (2)	K_2PtCl_4
Data collection											
X-ray source[1]	E	E	H	H	H	E	D	S	S	D	D
Wavelength (Å)	1.54	1.54	0.928	0.928	0.928	1.54	0.89	1.54	1.54	0.99	1.44
Resolution (Å)	2.1	2.3	1.98	2.4	2.4	3.2	2.0	3.98	3.98	2.22	4.2
Completeness (%)	86.1	93.3	98.0	96.7	99.6	99.6	96	99.7	99.7	98.9	92.2
R_{merge} (%)[2]	10.4	8.7	8.2	3.4	5.3	10.2	4.3	7.1	6.2	6.6	12.5
R_{iso} (%)[3]		20.8	16.0	25.5	29.3	14.6			15.8	10.5	23.9
MIR phasing											
Soak (mM/time)		5/3 h	3/1 day	3/1 day	5/1 day	3/3 days			1/1 min	0.1/5 min	1/5 min
No. of sites		8	5	6	7	4			1	1	1
Phasing power[4]		1.75	1.56	1.15	1.12	1.36			1.6	0.8	0.7

	Type I DHQase	Type II DHQase		Type I DHQase	Type II DHQase
Data			*Stereochemistry*		
Resolution (Å)	2.1	2.0	Ramachandran quality (%)		
R_{work} (%)	19.9	14.7	Most favored regions	92.5	97.3
R_{free} (%)	24.7	19.6	Allowed regions	7.5	2.7
No. of reflections:			R.m.s. deviation:		
Total	66,770	37,418	Bond length (Å)	0.010	0.014
Unique	23,517	11,412	Bond angle (°)	1.5	1.7

[1]D, Beamline 9.5 at the CCLRC Daresbury Laboratory, UK. S, Siemens X-1000 area detector (Glasgow). E, Enraf-Nonius FR571 generator, MAR image plate (Edinburgh). H, Stations X31 and X11 at EMBL Outstation, Hamburg.
[2]$R_{merge} = \sum_h (\sum_j |I_{j,h} - \langle I_h \rangle| / \sum I_{j,h})$, where h = reflection (hkl); j = all observations of reflection h.
[3]$R_{iso} = \sum_h ||F_{PH}| - |F_P|| / \sum_h |F_P|$, where $|F_{PH}|$, $|F_P|$ are observed derivative and native structure factor amplitudes, respectively.
[4]$[\sum_h |F_H|^2 / \sum_h |E|^2]^{1/2}$ where $|F_H|$ is the calculated heavy-atom structure factor amplitude and $\sum_h |E|^2 = \sum_h [|F_{PH}|^{obs} - |F_{PH}|^{calc}]^2$

included to a resolution of 2.18 Å using the merged native 1 and 2 data. Prior to the start of refinement, a set of 10% of the total reflections were assigned to calculate the R_{free} value. In the final stages of refinement solvent was fitted using ARP[39]. No electron density was obtained for amino acids 19–24, which are most likely to be disordered.

Coordinates. The coordinates for both structures have been deposited in the Protein Databank (accession code numbers 1qfe for type I DHQase and 2dhq for type II enzyme).

Acknowledgments
We thank S. Bury, B. Boys, A. Lapthorn, J. Milner-White, G. Murshudov and L.A.A. Meira for help at various stages of the work and the staff at the SRS Daresbury, Warrington, UK and the EMBL Outstation, DESY, Hamburg for providing data collection facilities. This work was supported by the Biotechnology and Biological Science Research Council.

Correspondence should be addressed to L.S. *email: L.Sawyer@ed.ac.uk* or J.R.C. *email: j.coggins@bio.gla.ac.uk*

Received 7 October, 1998; accepted 6 January, 1999.

1. Chaudhuri, S., Duncan, K., Graham, L. D. & Coggins, J. R. *Biochem. J.* **275**, 1–6 (1991).
2. Boys, C.W.G. *et al. J. Mol. Biol.* **227**, 352–355 (1992).
3. Banner, D.W. *et al. Nature* **255**, 609–614 (1975).
4. Sygusch, J., Beaudry, D. & Allaire, M. *Proc. Natl. Acad. Sci. USA* **84**, 7846–7850 (1987).
5. Izard, T., Lawrence, M.C., Malby, R.L., Lilley, G.G. & Colman, P.M. *Structure* **2**, 361–369 (1994).
6. Mirwaldt, C., Korndörfer, I. & Huber, R. *J. Mol. Biol.* **246**, 227–239 (1995).
7. Burnett, R.M. *et al. J. Biol. Chem.* **249**, 4383–4392. (1974).
8. Krell, T., Horsburgh, M.J., Cooper, A., Kelly, S.M. & Coggins, J.R. *J. Biol. Chem.* **271**, 24492–24497 (1996).
9. Jia, J., Schörken, U., Lindqvist, Y., Sprenger, G.A. & Schneider, G. *Protein Sci.* **6**, 119–124 (1997).
10. Reilly, A. *et al. J. Biol. Chem.* **269**, 5523–5526 (1994).
11. Deka, R.K., Kleanthous, C. & Coggins, J.R. *J. Biol. Chem.* **267**, 22237–22242 (1992).
12. Leech, A.P., James, R., Coggins, J.R. & Kleanthous, C. *J. Biol. Chem.* **270** 25827–25836 (1995).
13. Bottomley, J.R., Hawkins, A.R. & Kleanthous, C. *Biochem. J.* **319**, 269–278 (1996).
14. Harris, J.M., Gonzalez-Bello, C., Kleanthous, C., Hawkins, A.R, Coggins, J.R. & Abell,C. *Biochem. J.* **319**, 333–336 (1996).
15. Price, N.C. *et al. Biochem. J.* **338**, 195–202 (1999).
16. Hawkins, A.R., Lamb, H. K., Moore, J.D., Charles, I G. & Roberts, C.F. *J. Gen. Microbiol*. **139**, 2891–2899 (1993).
17. Giles, N.H. *et al. Microbiol. Rev.* **49**, 338–358 (1985).
18. Hawkins, A.R., Lamb, H.K., Smith, M., Keyte, J.W. & Roberts, C.F. *Mol. Gen. Genet*. **214**, 224–231 (1988).
19. Giles, N.H., Partridge, C.W.H., Ahmed, S.I. & Case, M.E. *Proc. Natl. Acad. Sci. USA* **58**, 1930–1937 (1967).
20. Hawkins, A.R., Giles, N.H. & Kinghorn, J.R. *Biochem. Genet*. **20**, 271–286 (1982).
21. Euverink, G.J.W., Hessels, J.W., Vrijbloed, J.W., Coggins, J.R. & Dijkhuizen, L. *J. General. Microbiol*. **138**, 2449–2457 (1992).
22. Philipp, W.J. *et al. Proc. Natl. Acad. Sci. USA* **93**, 3132–3137 (1996).
23. Tomb, J.F. *et al. Nature* **388**, 539–547 (1997).
24. Lamb, H.K. *et al. Biochem.J.* **313**, 941–950 (1996).
25. Haslam, E. *Shikimic acid: metabolism and metabolites* (J. Wiley & Sons, Chichester, England; 1993).
26. Mousdale, D.M. & Coggins, J.R. (1991) In *Target sites for herbicide action* (ed. Kirkwood, R. C.) 29–56 (Plenum Press, New York; 1991).
27. Balasubramanian, S.G.M., Davies, G.M., Coggins, J.R. & Abell, C. *J. Am. Chem. Soc*. **113**, 8945–8946 (1991).
28. Davies, G.M. *et al. Antimicrob. Agents Chemother.* **38**, 403–406 (1994).
29. Tacket, C.O. *et al. Vaccine* **10**, 443–446 (1992).
30. Karnell, A. *et al. Vaccine* **11**, 830–836 (1993).
31. Otwinowski, Z. & Minor, W. *Methods. Enzymol*. **276**, 307–326 (1997).
32. Collaborative Computational Project, Number 4. *Acta Crystallogr. D* **50**, 760–763 (1994).
33. Brünger, A. T. *X-PLOR Manual version 3.1: A system for crystallography and NMR*. (Yale University Press, New Haven, Connecticut; 1992).
34. Otwinowski, Z. In *Isomorphous replacement and anomalous scattering*. (eds. Wolf, W. Evans, P.R. & Leslie, A.G.W.) 80–85 (SERC Daresbury Laboratory, Warrington, UK; 1991).
35. Cowtan, K. *Joint CCP4 and ESF-EACBM Newsletter on protein crystallography.* **31**, 24–28 (1994).
36. Jones, T.A., Zou, J.-Y., Cowan, S. W. & Kjelgaard, M. *Acta Crystallogr. A* **47**, 110–119 (1991).
37. Gourley, D.G. *et al. J. Mol. Biol.* **241**, 488–491 (1994).
38. Murshudov, G.N., Dodson, E.J. & Vagin, A.A. In *Macromolecular refinement* (eds Dodson, E., Moore, M. & Bailey, S.) 93–104 (SERC Daresbury Laboratory, Warrington, UK; 1996).
39. Lamzin, V.S. & Wilson, K.S. *Acta Crystallogr. D* **49**, 129–147 (1993).
40. Kraulis, P.J. *J. Appl. Crystallogr.* **24**, 946–950 (1991).